Analytica Chimica Acta xxx (2017) 1–10

Contents lists available at ScienceDirect

Analytica Chimica Acta

journal homepage: www.elsevier.com/locate/aca

Microfluidic immunosensor based on mesoporous silica platform and CMK-3/poly-acrylamide-*co*-methacrylate of dihydrolipoic acid modified gold electrode for cancer biomarker detection

Matías Regiart [b], Martin A. Fernández-Baldo [a], Jhonny Villarroel-Rocha [b], Germán A. Messina [a], Franco A. Bertolino [a], Karim Sapag [b], Aaron T. Timperman [c, *], Julio Raba [a, **]

[a] INQUISAL, Departamento de Química, Universidad Nacional de San Luis, CONICET, Chacabuco 917, D5700BWS, San Luis, Argentina
[b] INFAP, Laboratorio de Sólidos Porosos, Universidad Nacional de San Luis, CONICET, Ejercito de los Andes 950, D5700BWS, San Luis, Argentina
[c] Advanced Diagnostics & Therapeutics, Department of Chemistry and Biochemistry, University of Notre Dame, Notre Dame, IN 46556, USA

HIGHLIGHTS

- A microfluidic immunosensor has been developed for epidermal growth factor receptor (EGFR) in human serum samples.
- In this immunoassay, the anti-EGFR antibodies are immobilized on a surface area amino mesoporous silica as platform.
- The gold electrodes are coated with CMK-3/poly-acrylamide-co-methacrylate of dihydrolipoic acid nanocomposite.
- The sensor's linear range is from 0.01 to 50 ng mL^{-1} with a single day RSD of 4.98%.

GRAPHICAL ABSTRACT

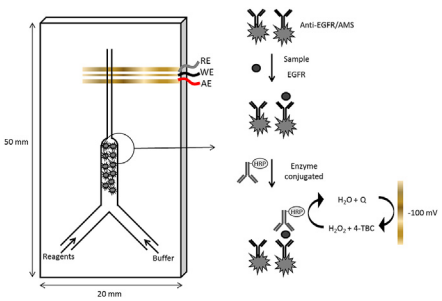

ARTICLE INFO

Article history:
Received 10 November 2016
Received in revised form
29 December 2016
Accepted 19 January 2017
Available online xxx

Keywords:
EGFR
Cancer biomarker
Cancer diagnosis
Mesoporous silica

ABSTRACT

We report a hybrid glass-poly (dimethylsiloxane) microfluidic immunosensor for epidermal growth factor receptor (EGFR) determination, based on the covalent immobilization of anti-EGFR antibody (anti-EGFR) on amino-functionalized mesoporous silica (AMS) retained in the central channel of a microfluidic device. The synthetized AMS was characterized by N_2 adsorption-desorption isotherm, scanning electron microscopy (SEM), energy dispersive spectrometry (EDS) and infrared spectroscopy. The cancer biomarker was quantified in human serum samples by a direct sandwich immunoassay measuring through a horseradish peroxidase-conjugated anti-EGFR. The enzymatic product was detected at −100 mV by amperometry on a sputtering gold electrode, modified with an ordered mesoporous carbon (CMK-3) in a matrix of poly-acrylamide-*co*-methacrylate of dihydrolipoic acid (poly(AC-*co*-MDHLA)) through *in situ* copolymerization. CMK-3/poly(AC-*co*-MDHLA)/gold was characterized by cyclic voltammetry, EDS and SEM. The measured current was directly proportional to the level of EGFR in human serum samples. The linear range was from 0.01 ng mL^{-1} to 50 ng mL^{-1}. The detection limit was

* Corresponding author. Department of Chemistry and Biochemistry, University of Notre Dame, 311-I Cushing Hall, Notre Dame, IN 46556, USA.
** Corresponding author.
E-mail addresses: atimperm@nd.edu (A.T. Timperman), jraba@unsl.edu.ar (J. Raba).

http://dx.doi.org/10.1016/j.aca.2017.01.029
0003-2670/

Microfluidic immunosensor
Nanostructured electrode

3.03 pg mL^{-1}, and the within- and between-assay coefficients of variation were below 5.20%. The microfluidic immunosensor is a very promising device for the diagnosis of several kinds of epithelial origin carcinomas.

1. Introduction

Epidermal growth factor receptor (EGFR, ErbB1; HER1) is a cell *trans*-membrane protein located on the cell surface, that is activated by binding to their specific ligands, such as epidermal growth factor and transforming growth factor, which activates the tyrosine kinase in its intracellular domain and induces intracellular signaling pathways that control relevant cellular processes, including adhesion, migration, apoptosis, cell differentiation and proliferation [1,2]. Overexpression of EGFR protein has been reported in several kinds of epithelial origin carcinomas, such as breast, lung, head/neck, gastric, colorectal, renal, prostate, esophageal, ovarian, and pancreatic cancers [3,4]. Furthermore, the increased expression of EGFR is linked to an increased rate of proliferation, increased invasiveness and a high mortality prognostic. Hence, there is increasing interest in the quantification of EGFR levels, both for diagnosis and prognosis as an indicator associated with more aggressive and resistant to treatment tumors [5,6].

Conventional techniques for EGFR determination include enzyme-linked immunosorbent assay (ELISA) of intact cells [7,8], western blotting of cell lysate [9,10], and immunohistochemistry on tumor tissue samples [11,12]. However, these methods are technically demanding, time consuming and require highly qualified personnel. Thus, the development of a sensitive, selective, simple, rapid, and inexpensive method for detecting cancer biomarkers in real samples is critical.

To improve the detection of EGFR, the sample delivery and sample preparation capabilities of microfluidic devices have been utilized to greatly increase the speed of EGFR detection using immunostaining of whole cells. These devices capture cells above a track-etched membrane and stain the cells before characterization using fluorescence microscopy [17,18]. Recently, the electrochemical immunosensors have become more important for the detection of cancer biomarkers [13,14], due to the electrochemical detection provides the required limits of detection, selectivity, rapid analysis times, and faster data analysis than immunostaining methods. These electrochemical immunosensors can be readily incorporated into microfluidic devices, which offer several useful properties including low sample and reagent consumption, high sensitivity, fast response, portability, ease of use and short time for analysis [15,16].

Of the numerous methods available to fabricate microfluidic devices, the hybrid glass-poly (dimethylsiloxane) (PDMS) microfluidic devices are particularly well-suited for integration of electrochemical devices. The glass substrate provides a support that is thermally stable and amenable to deposition of the electrodes by sputtering. PDMS based microfabrication methods are well-established and provide an inexpensive method for rapid reproduction of the layer with patterned substrates. Therefore, these hybrid devices utilize the best attributes of both substrates and also have the advantages of: low cost, durability, chemical inertness, optical transparency, and automation capacity [19,20]. In addition, electrochemical detection allows great versatility, which can be easily incorporated into a portable device. The gold electrodes do not require vapor deposition and can be easily sputtered on the glass [21,22].

To improve the limit of detection several publications reported the use of simple/multiwalled carbon nanotubes, graphene, carbon nanofibers among others [23,24]. These materials have unique electric, electrocatalytic and mechanical properties, which make them efficient materials for developing electrochemical immunosensors. However, we increased the surface area of the gold electrode through *in situ* copolymerization and deposition of an ordered mesoporous carbon (CMK-3) in a matrix of poly-acrylamide-*co*-methacrylate of dihydrolipoic acid (Poly(AC-*co*-MDHLA)). CMK-3 has been used in different applications due to the periodically mesoporous structure, high specific surface area, large pore volume, and tunable pore size distribution [25]. These materials have been widely used, because of their fast electron transfer, high surface area, and excellent electrocatalytic activity, avoiding surface fouling. The excellent electrocatalytic properties of modified electrodes with ordered mesoporous carbons have been reported [26]. Furthermore, the poly(AC-*co*-MDHLA) has thiol functional groups that bind strongly to gold, thereby obtaining a highly stable electrode under extreme conditions of salt and pH [27].

In the last years, different materials have been incorporated into electrochemical immunosensors as immobilization supports for the specific immunoreactants. One the most commonly used solid supports are the different kinds of porous silica materials [28,29]. These porous silica materials have many benefits, such as the increase of the surface to volume ratio that increases interactions between the immunoreagents and EGFR and lowers the limits of detection [30,31]. We synthetized, functionalized, characterized and used an amino mesoporous silica (AMS) as immobilization platform for the anti-EGFR antibody (anti-EGFR). AMS has an increased surface and uniform porous, compared with the commercial 3-aminopropyl modified controlled pore glass (AP-CPG) normally used as immobilization support.

In the present work, we developed a hybrid glass-PDMS microfluidic electrochemical immunosensor for EGFR determination, based on the covalently immobilization of anti-EGFR on AMS retained in the central channel (CC) of the microfluidic device. AMS was characterized by N_2 adsorption-desorption isotherm, scanning electron microscopy (SEM), energy dispersive spectrometry (EDS), and infrared spectroscopy (FTIR). The cancer biomarker was quantified by a direct sandwich immunoassay measuring through a horseradish peroxidase (HRP)-conjugated anti-EGFR. The enzymatic product (benzoquinone) was detected by reduction at −100 mV by amperometry on a sputtering gold electrode modified with CMK-3 in a matrix of poly(AC-*co*-MDHLA) through *in situ* copolymerization. CMK-3/poly(AC-*co*-MDHLA)/gold was characterized by cyclic voltammetry (CV), EDS and SEM. The measured current was directly proportional to the level of EGFR in human serum samples. To the best of our knowledge, no study involving a microfluidic electrochemical immunosensor with an own design, using AMS as immobilization platform for EGFR determination in biological samples has been reported being this the novelty of our work. The microfluidic immunosensor is a very promising device for the diagnosis of several kinds of epithelial origin carcinomas.

Please cite this article in press as: M. Regiart, et al., Microfluidic immunosensor based on mesoporous silica platform and CMK-3/poly-acrylamide-*co*-methacrylate of dihydrolipoic acid modified gold electrode for cancer biomarker detection, Analytica Chimica Acta (2017), http://dx.doi.org/10.1016/j.aca.2017.01.029

2. Experimental

2.1. Materials and reagents

All reagents used were of analytical reagent grade. Sylgard 184, including PDMS prepolymer and curing agent, and SU-8 photoresist were obtained from Dow Corning (Midland, MI, USA) and Clariant Corporation (Sommerville, NJ, USA), respectively. Glutaraldehyde (25% aqueous solution), *N*,*N*-dimethylacetamide (DMA), methanol, ethanol, toluene, tetraethyl orthosilicate (TEOS 98%), and 3-aminopropyl triethoxysilane (3-APTES) were purchased from Merck (Darmstadt, Germany). Bovine serum albumin (BSA), sodium borohydride ($NaBH_4$, 99.99%), hydrofluoric acid (HF), 2-cyano-2-propyl dodecyl trithiocarbonate (CPDT), 4,4′-Azobis(4-cyanovaleric acid) (ACVA), acrylamide (AC), and 4-*tert*-butylcatechol (4-TBC) were purchased from Sigma-Aldrich (St. Louis, MO, USA). Methacrylate of lipoic acid (MLA) was prepared according to literature procedure by the carbodiimide coupling of hydroxyethyl methacrylate and lipoic acid [27]. The commercial ELISA kit (enzyme immunoassay) for the quantitative determination of EGFR biomarker was purchased from Cloud-Clone Corp. (Houston, USA), and it was used according to the manufacturer's instructions. Monoclonal anti-EGFR antibody and HRP-conjugated anti-EGFR were purchased from Abcam® (USA). All the other employed reagents were of analytical grade and were used without further purification. Aqueous solutions were prepared by using purified water from a Milli-Q system.

2.2. Apparatus

The amperometric detection and voltammetric characterization were performed with a BAS LC-4C Electrochemical Detector, and a BAS 100B/W Electrochemical Workstation (Bioanalytical Systems, Inc. West Lafayette, IN, USA), respectively. Electrochemical measurements were carried out using a microfabricated gold electrochemical cell with three electrodes (gold working electrode modified with CMK-3/poly(AC-*co*-MDHLA)). All the potentials in the text were referred to gold. Scanning electron microscope images were taken on a LEO 1450VP (UK), equipped with an Energy Dispersive Spectrometer analyzer, Genesis 2000 (England). Infrared (FTIR) spectroscopic measurements were obtained in a Spectrum 65 FI IR spectrometer Perkin Elmer, in a region from 4000 to 400 cm^{-1}. Textural characterization was carried out by N_2 adsorption-desorption isotherms at 77 K using a manometric adsorption equipment (ASAP 2000, Micromeritics), where the samples were previously degassed at 60 °C for 20 h, up to a residual pressure smaller than 2 Pa.

A syringe pumps system (Baby Bee Syringe Pump, Bioanalytical Systems, Inc. West Lafayette, IN, USA) was used for introducing the solutions in the device. All solutions and reagent temperatures were conditioned before the experiment using a Vicking Masson II laboratory water bath (Vicking SRL, Buenos Aires, Argentina). Absorbance was detected by Bio-Rad Benchmark microplate reader (Japan) and Beckman DU 520 general UV/VIS spectrophotometer. All pH measurements were made with an Orion Expandable Ion Analyzer (Orion Research Inc., Cambridge, MA, USA) Model EA 940 equipped with a glass combination electrode (Orion Research Inc).

2.3. Microfluidic device fabrication

The microfluidic device fabrication involved the following steps: i) Sputtering deposition of the electrodes (Ag/Au) on a glass plate, ii) Fabrication of the PDMS molds with photolithography and, iii) Immobilization of CMK-3 modified with poly(AC-*co*-MDHLA) through *in situ* polymerization on gold electrode, and iv) Sealing of the glass/PDMS device as shown in Scheme 1. The construction of microfluidic immunosensor was carried out according to the procedure proposed by Moraes et al. with the following modifications [20]. Scheme 2 shows a schematic of the microfluidic immunosensor, whose design consisted of a Y-configuration (two inlets for reagents and buffer, respectively, and one outlet) with 250-μm-width and 150-μm-height, with a central channel (CC) (40 mm length, decreased from 250 to 100-μm-width and from 150 to 100-μm-height).

A mask designed of self-adhesive vinyl sheet patterned using a blade cutter was employed for the construction of the electrodes. The mask was positioned at the end of the CC and a 20 nm adhesion layer of silver followed by 100 nm of gold, was deposited over a glass plate by sputtering (SPI-Module Sputter Coater, Structure Probe Inc, West Chester, PA). The thickness of the gold electrode was controlled using a Quartz Crystal Thickness Monitor model 12161 (SPI-Module, Structure Probe Inc, West Chester, PA) (Scheme 2). The vinyl mask was removed after sputtering, leaving the gold tracks on the glass. The geometric areas of the electrodes are 1.0 mm^2 for the working electrode and 2.0 mm^2 for counter and reference electrodes.

As illustrated in Scheme 1, the microchannels in the PDMS were cast by photolithography [32]. The design of the channels in the negative mask was generated by a computer drawing program. The replication master was patterned with a SU-8 photoresist layer over a silicon wafer using a spin coater at 2000 rpm for 30 s, and baked at 65 °C for 2 min and 95 °C for 6 min. Then, the coated sheet was

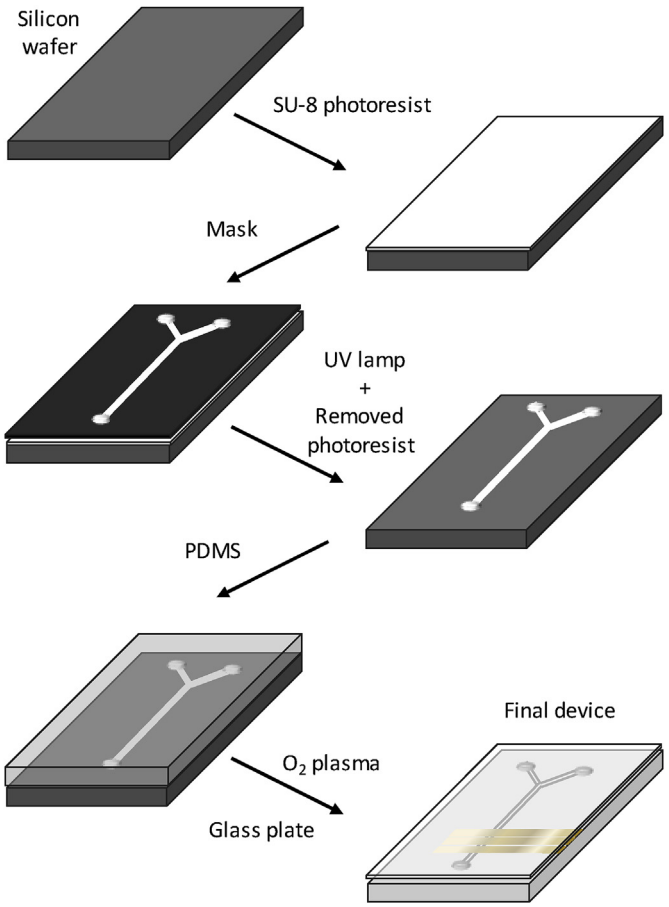

Scheme 1. Fabrication and assembly of the hybrid microfluidic device using photolithography to pattern a mold for the casting the PDMS layer containing the microchannels and a glass slide with patterned electrodes.

Please cite this article in press as: M. Regiart, et al., Microfluidic immunosensor based on mesoporous silica platform and CMK-3/polyacrylamide-*co*-methacrylate of dihydrolipoic acid modified gold electrode for cancer biomarker detection, Analytica Chimica Acta (2017), http://dx.doi.org/10.1016/j.aca.2017.01.029

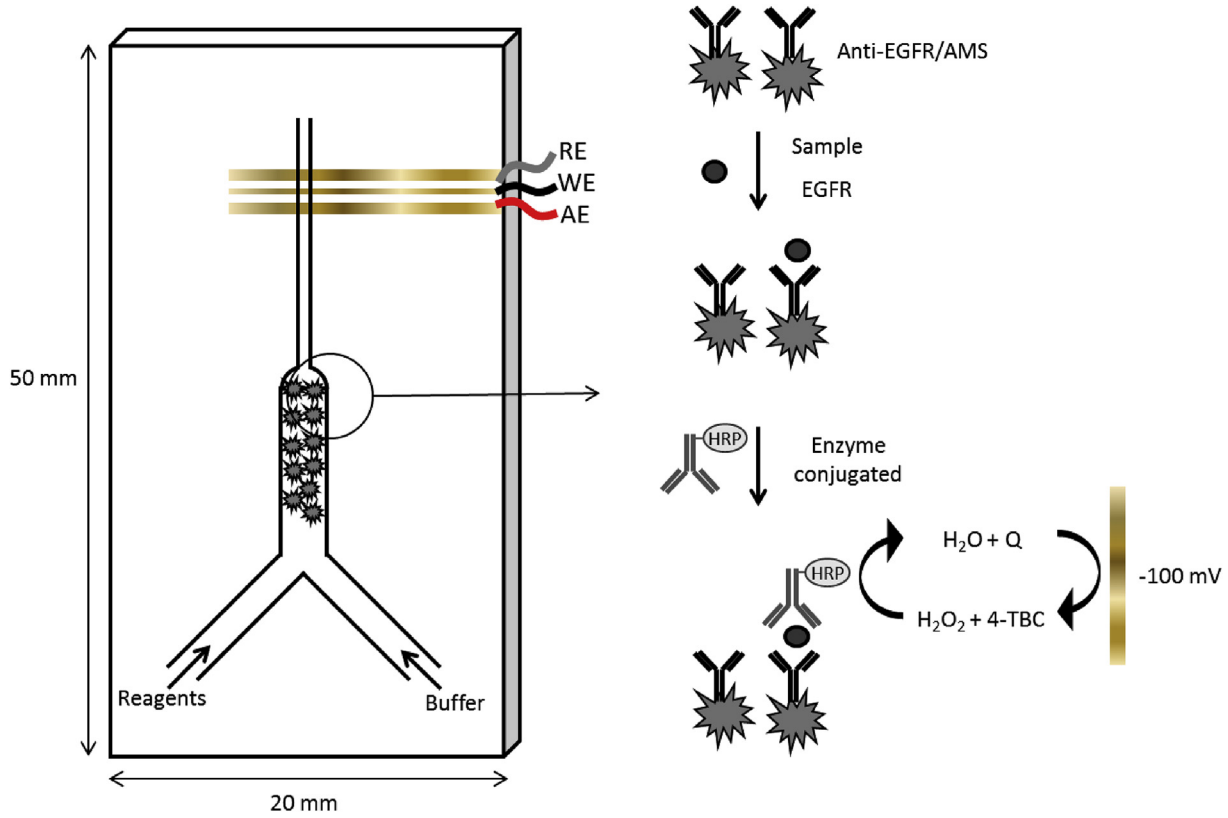

Scheme 2. An illustration showing the major steps for the determination of EGFR in human serum samples: 1) antibody conjugated to the AMS particles are loaded into the microchannel microfluidic channel, 2) serum sample (diluted 100:1 in PBS) is passed through the microfluidic channel, 3) EGFR binds to the antibody, 4) secondary antibody is passed through the microchannel and binds to the EGFR 5) 4-*tert*-butylcatechol is oxidized to benzoquinone and 6) benzoquinone is reduced to 4-*tert*-butylcatechol at the electrode surface.

exposed to UV lamp through a negative mask design containing the desired channel. After that, the unexposed photoresist was removed, the Sylgard curing agent and PDMS prepolymer were mixed in a 1:10 wt ratio and the mixture was placed on the replication master and degassed for 30 min to eliminate air bubbles. The polymer curing process was carried out in a hot plate at 65 °C for 1 h, and the cured PDMS layer was peeled from the replication master. The external access to the microfluidic device was obtained by drilling holes in the PDMS. After the gold electrode modification with the CMK-3/poly(AC-*co*-MDHLA), the glass plate and PDMS were placed in oxygen plasma for 1 min, and were contacted immediately for a strong seal.

2.4. Synthesis of CMK-3/poly(AC-co-MDHLA) by in situ copolymerization

CMK-3 was synthesized using the ordered mesoporous material SBA-15 as inorganic template and sucrose as carbon source by means of a nanocasting technique based on the procedure reported by Barrera et al. (2013) [33], as can be seen in A1, A2. In addition, to achieve the CMK-3 functionalization, a chemical treatment using a mixture of concentrated acids H_2SO_4:HNO_3 (3:1) for 12 h was carried out. After this step, the suspension was filtered; the solid was washed with ultrapure water at pH 7.00 and dried at 120 °C for 5 h.

The nanocomposite CMK-3/poly(AC-*co*-MDHLA) was synthesized using a typical reaction procedure, with the following modifications [34]. In a Pyrex tube containing 5 mL of Methanol:DMA (3:2) were added 1 g of CMK-3, 2.00 g of a 50% mixture of monomers (MLA + AC), 0.02 g of CPDT and 0.01 g of ACVA, in a ratio of monomers:RAFT:initiator (100:1:0.5). The tube was degassed using N_2 for 30 min. Then, the mixture reacted in a thermostatic bath at 70 °C under stirring for 12 h, and the polymerization was stopped by cooling the tube. Poly(AC-*co*-MLA) copolymer was reduced by $NaBH_4$ solution in H_2O:Methanol (2:1) at 0 °C for 3 h (Fig. A3). Later, the supernatant was centrifuged for 6 h and vacuum-filtered through a 0.20 μm PTFE membrane. To obtain the dispersion of the nanocomposite CMK-3/poly(AC-*co*-MDHLA), the following procedure was employed: 10 mg was dispersed in 1 mL DMF and ultrasonicated for 2 h in order to obtain a homogeneous suspension. An aliquot of 2 μL of this dispersion was added to the gold electrode, and the solvent was evaporated under the action of an infrared heat lamp.

2.5. Synthesis of AMS

The mesoporous silica (MS) was synthesized according to the procedure described by Einarsrud et al. (1998) [35] with the following modifications, where the silica was prepared with TEOS:H_2O:ethanol:HCl:NH_4OH ($1:3.5:3.9:7.8 \times 10^{-4}:5.78 \times 10^{-3}$). First, the TEOS was hydrolyzed (initial hydrolysis) in an aqueous/alcoholic solution with TEOS:H_2O:ethanol:HCl ($1:1:3.9:7.8 \times 10^{-4}$). This mixture was stirred under reflux at 60 °C for 1.5 h, and then the NH_4OH and the remaining H_2O were added to this solution (for final hydrolysis). The resulting solution was gelled at 45 °C for 24 h without stirring. Subsequently, the gel was aged at 85 °C for 24 h. The solid was ground, washed with a mixture of H_2O/ethanol (50:50 v/v) until the conductivity of the wash solution was less than 10 μS cm^{-1}, and dried at 60 °C for 12 h.

AMS was prepared according to the procedure described above, with some modifications [36]. 7 mL of APTES (30 mmol) was added

Please cite this article in press as: M. Regiart, et al., Microfluidic immunosensor based on mesoporous silica platform and CMK-3/poly-acrylamide-*co*-methacrylate of dihydrolipoic acid modified gold electrode for cancer biomarker detection, Analytica Chimica Acta (2017), http://dx.doi.org/10.1016/j.aca.2017.01.029

to 2.00 g of MS dispersed in 150 mL of toluene under N_2 flowing and vigorous stirring. Then, the mixture was refluxed at 100 °C for 6 h. Finally, the solid was filtered and washed with toluene followed by ethanol, and dried at 60 °C for 12 h.

2.6. Immobilization of the anti-EGFR in the AMS

To carry out the monoclonal anti-EGFR antibodies immobilization process, 1 mg of AMS in an eppendorf tube was allowed to react with 1 mL of an aqueous solution of 5% w/w glutaraldehyde (100 mM sodium phosphate buffer, pH 8.00) with continuous mixing for 2 h at room temperature. After three washes with 10 mM phosphate buffer saline pH 7.20 (PBS), 250 μL of antibody preparation (dilution 1:100 in 10 mM PBS pH 7.20) was coupled to the residual aldehyde groups with continuous mixing for 12 h at 5 °C. The immobilized antibody preparation was finally washed three times with PBS (10 mM pH 7.20) and stored in the same buffer at 5 °C. The anti-EGFR/AMS was perfectly stable for at least 1 month.

2.7. Analytical procedure for EGFR determination

The procedure for the quantification of EGFR involves the following steps. The suspension of anti-EGFR/AMS was injected using a syringe pumps at a flow rate of 10 μL min^{-1} for 5 min, and was packed into the CC. The carrier buffer was 10 mM PBS pH 7.20. The following solutions were injected at a flow rate of 2 μL min^{-1}. Firstly, the immunosensor was exposed to a desorption buffer (100 mM glycine-HCl pH 2.00) for 5 min and then was rinsed with 10 mM PBS pH 7.20 for 4 min. This treatment was carried out in order to desorb the immune-complex and start with a new analysis. Unspecific binding was blocked with 1% BSA in 10 mM PBS pH 7.20 by a 5 min treatment at room temperature and then was rinsed with 10 mM PBS pH 7.20 for 4 min. After that, the healthy human serum sample spiked with EGFR at concentrations shown in Table 2 (diluted 100-fold with 10 mM PBS pH 7.20) was injected into the PBS carrier stream for 5 min. Once the EGFR biomarker was recognized and captured by anti-EGFR immobilized on AMS. The microfluidic device was washed with 10 mM PBS pH 7.20 for 4 min to remove excess of sample. Later, the HRP-conjugated anti-EGFR (diluted 1000-fold with 10 mM PBS pH 7.20) was added for 5 min followed by a washing procedure with 10 mM PBS pH 7.20 for 4 min. Finally, the substrate solution (1 mM H_2O_2 + 1 mM 4-TBC in 10 mM phosphate-citrate buffer pH 5.00) was pumped and the enzymatic product was detected at −100 mV by amperometry (Voltammogram of 4-TBC in Fig. A4) (Scheme 2). The device could be used with no significant loss of sensitivity for 20 days, whereas its useful lifetime was one month with a sensitivity decrease of 10%. The storage of the microfluidic immunosensor was made in 10 mM PBS pH 7.20 at 5 °C.

3. Results and discussion

3.1. Characterization of AMS

The synthetized AMS was compared with MS, and a commercial 3-aminopropyl modified controlled pore glass (AP-CPG), as can be seen in Table 1. The specific surface area (S_{BET}) was estimated by the Brunauer, Emmet and Teller (*BET*) method [37], using the adsorption data in the range of relative pressures from 0.05 to 0.22. The micropore volume ($V_{\mu P}$) was calculated by the α_S-plot method [38] using the LiChrospher Si-1000 macroporous silica gel as the reference adsorbent. The total pore volume (V_{TP}) was determined by the Gurvich's rule at a relative pressure of 0.98 [39]. The mesopore size distribution (PSD) was obtained by the *VBS* macroscopic method [40] using the adsorption branch data.

As shown in Fig. 1A) the SEM of the AMS is composed of irregular particles with an average size of 150 μm. In the EDS of the AMS it can be observed the characteristic peak of silica (Fig. 1B). Fig. 1C) demonstrates the N_2 adsorption-desorption isotherm at 77 K of the AMS, MS and AP-CPG, respectively. MS and AMS present a Type IV isotherm and has a hysteresis loop H2 types, which are typical of mesoporous materials. The textural properties, obtained from adsorption data, shows the higher surface area of the AMS in comparison with the AP-CPG, whose direct consequence is the increment of the assays sensitivity, because of the higher quantity of antibodies which can bind to the silica surface. Moreover, Fig. 1C) (inset) shows an AMS uniform pore size distribution with a mesopore width around of 4.4 nm. In the FTIR measurements, it can be observed the changed between the MS and AMS in the peaks Si-OH (965), C-N, Si-O-Si, Si-CH_2-R (1220), -OH (3500), H-O-H (1645), N-H (690), NH_3^+ (1555), Si-O-Si (800), Si-O-Si (460) (Fig. 1D).

3.2. Characterization of the CMK-3/poly(AC-co-MDHLA)/gold electrode surface

Morphology of CMK-3/poly(AC-*co*-MDHLA)/gold nanocomposite film was investigated by SEM. Fig. 2A) reveals the homogeneous surface of CMK-3/poly(AC-*co*-MDHLA) polymerized over the gold electrode. In addition, the inset in Fig. 2A) shows the CMK-3 micrometer rod-like particles. The three-dimensional structure of CMK-3/poly(AC-*co*-MDHLA) nanocomposite film provides a suitable surface for a conductive pathway for electron-transfer. The elemental composition of the nanocomposite was determined by EDS. Fig. 2B) shows five peaks, corresponding to the C, O, Si, Au, and Ag elements, respectively.

CV of $[Fe(CN)_6]^{3-}/[Fe(CN)_6]^{4-}$ couple is a convenient and valuable tool to monitor the surface properties of the electrode during the different modification steps. Fig. 3A) shows the voltammograms following: (a) blank solution, (b) bare gold and (c) CMK-3/poly(AC-*co*-MDHLA)/gold, which were recorded in 1 mM $[Fe(CN)_6]^{3-}/[Fe(CN)_6]^{4-}$ in 100 mM KCl (Scan rate = 75 mV s^{-1}). Well-defined cyclic voltammograms and characteristics of a diffusion-controlled redox process were observed at the bare gold surface. When CMK-3/poly(AC-*co*-MDHLA) was immobilized on the gold surface, the redox peak current and background current at this

Table 1
Textural properties of AMS and AP-CPG.

Material	$S_{BET}/m^2 \cdot g^{-1}$	$V_{\mu P}/cm^3 \cdot g^{-1}$	$V_{TP}/cm^3 \cdot g^{-1}$
AMS[a]	490 (900)	0 (0.01)	0.34 (0.65)
AP-CPG	16	0	0.02

[a] Values in parenthesis correspond to mesoporous silica without modification.

Table 2
Comparison of EGFR concentration in human serum samples by microfluidic immunosensor (MI) and ELISA.

Samples[a]	Standard addition	EGFR (ng mL^{-1})	
		MI[b]	ELISA
SS 1	0	1.32 + 0.02[c]	1.33 + 0.03
SS 2	5	7.95 + 0.07	7.33 + 0.05
SS 3	10	15.14 + 0.05	15.88 + 0.06
SS 4	25	31.19 + 0.09	30.23 + 0.08
SS 5	45	48.13 + 0.11	48.97 + 0.14

[a] Human serum samples.
[b] Microfluidic immunosensor.
[c] Mean of three determinations + S.D.

Please cite this article in press as: M. Regiart, et al., Microfluidic immunosensor based on mesoporous silica platform and CMK-3/poly-acrylamide-*co*-methacrylate of dihydrolipoic acid modified gold electrode for cancer biomarker detection, Analytica Chimica Acta (2017), http://dx.doi.org/10.1016/j.aca.2017.01.029

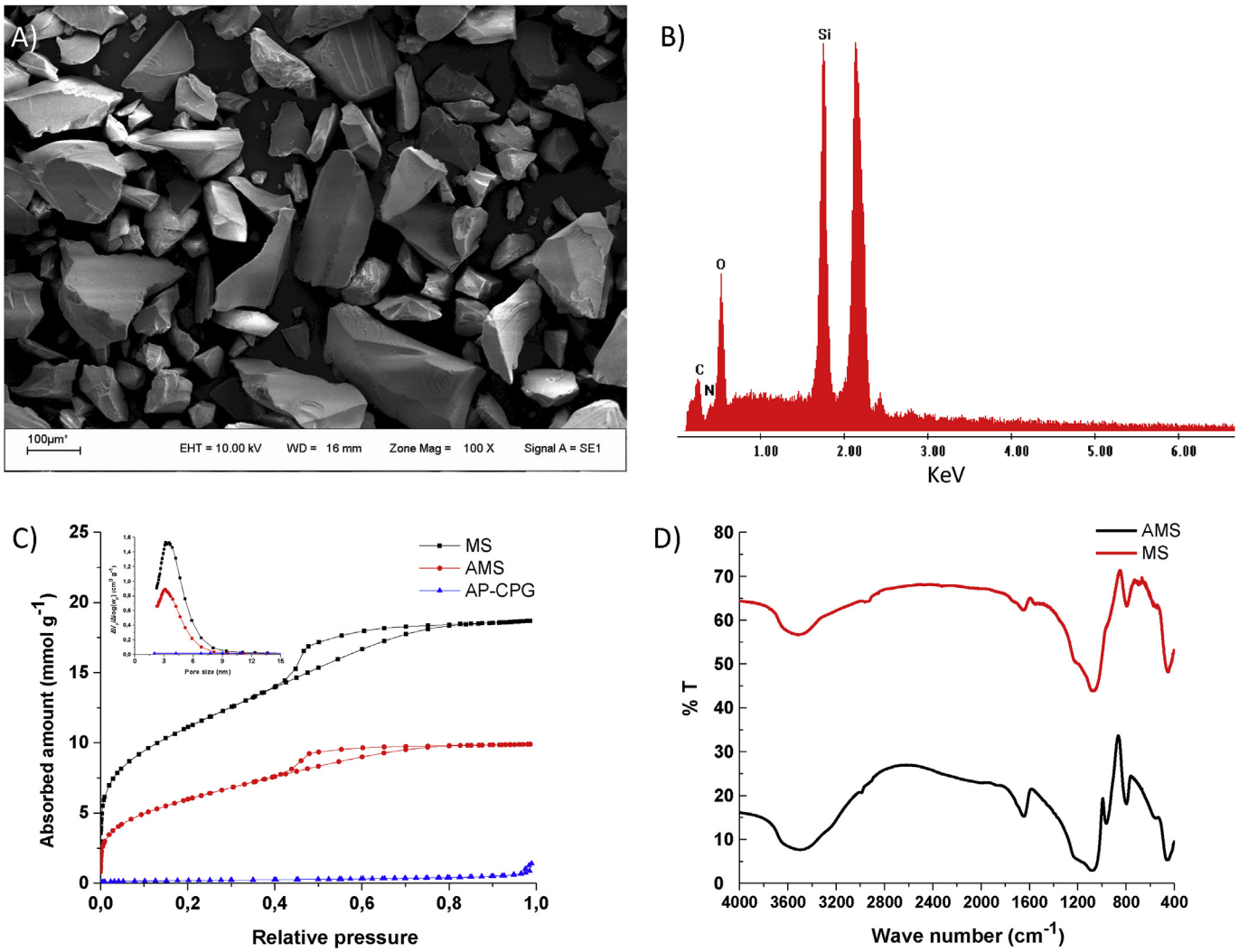

Fig. 1. A) SEM micrograph of AMS, B) EDS microanalysis of AMS, C) N_2 adsorption-desorption isotherms of MS, AMS and AP-CPG at 77 K, (insetted) mesopore size distribution of materials under study, and D) FTIR measurements of MS, AMS, and AP-CPG.

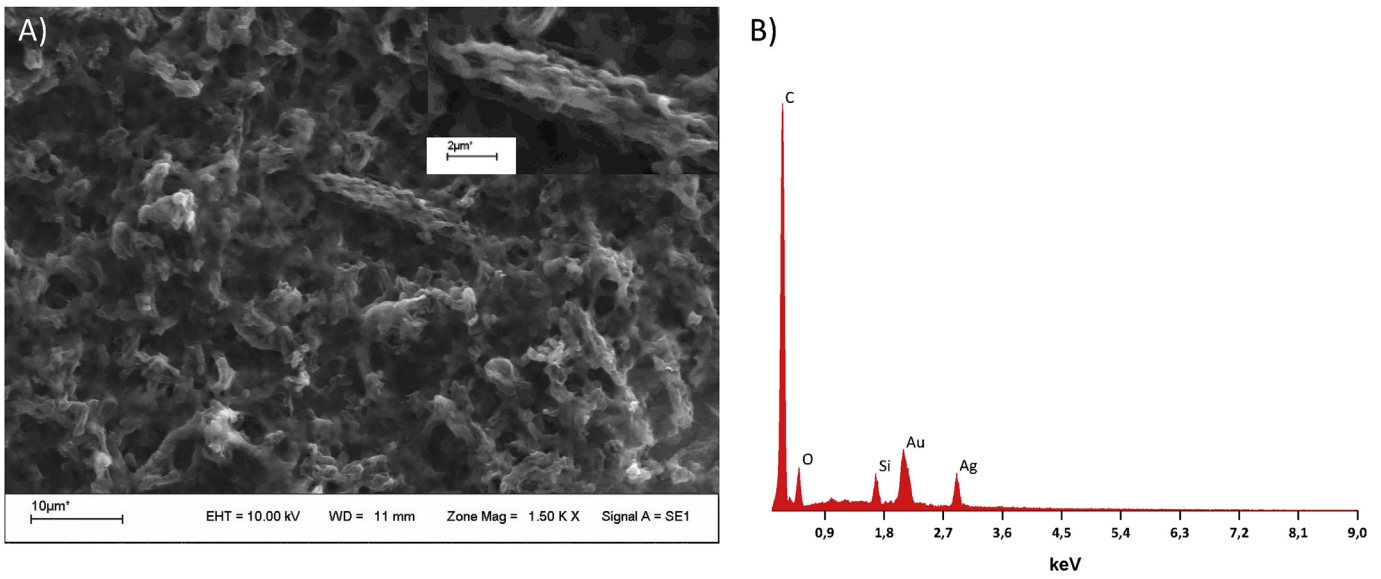

Fig. 2. A) SEM micrograph of CMK-3/poly(AC-*co*-MDHLA)/gold nanocomposite, and B) EDS microanalysis of the nanocomposite.

Please cite this article in press as: M. Regiart, et al., Microfluidic immunosensor based on mesoporous silica platform and CMK-3/poly-acrylamide-*co*-methacrylate of dihydrolipoic acid modified gold electrode for cancer biomarker detection, Analytica Chimica Acta (2017), http://dx.doi.org/10.1016/j.aca.2017.01.029

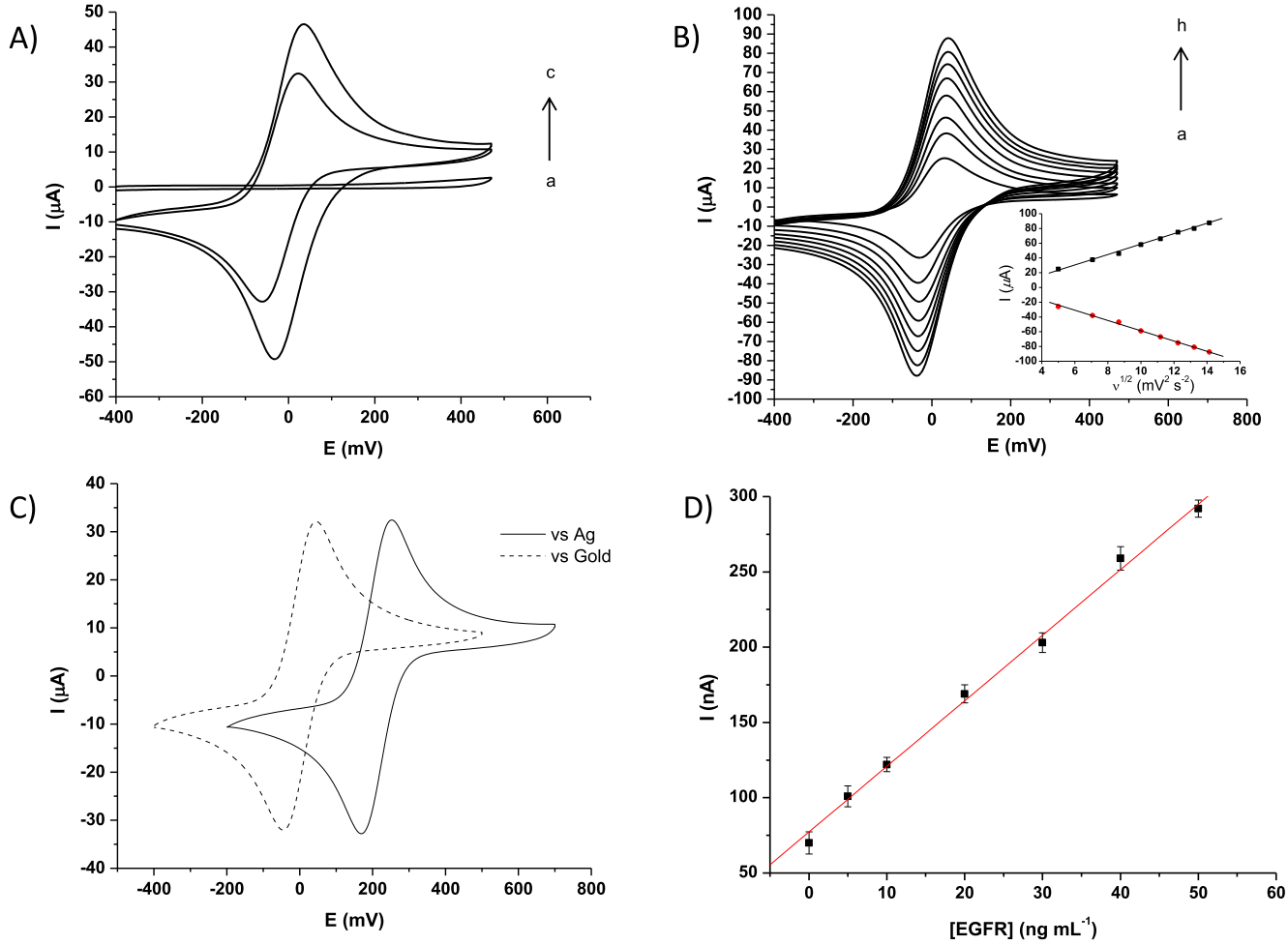

Fig. 3. A) CV for: (a) blank solution, (b) bare gold and (c) CMK-3/poly(AC-*co*-MDHLA)/gold, recorded in 1 mmol L^{-1} $[Fe(CN)_6]^{3-}/[Fe(CN)_6]^{4-}$ in 0.1 mol L^{-1} KCl (Scan rate = 75 mV s^{-1}), B) Current of redox peak vs square roots of ν from 25 to 200 mV s^{-1}, C) The gold pseudo reference electrode showed a cathodic shift of potential of 205 mV when compared with the Ag/AgCl reference electrode, and D) Calibration curve described according to the following equation: ΔI (nA) = 77.26 + 4.35 [EGFR] (ng mL^{-1}) with a correlation coefficient of R: 0.998.

modified electrode were both enlarged, which demonstrated the increase of faradaic and non-faradaic residual currents. These phenomena may be attributed to two factors: firstly, the excellent electrical conductivity of CMK-3, secondly, the increase electroactive surface area and more electrocatalytic sites of this detection platform. Moreover, the poly(AC-*co*-MDHLA) allows the union of the nanocomposite with the gold surface owing to thiols groups of the polymer, thereby obtaining a highly stable modified electrode. The great advantage of the nanocomposite is that it prevents fouling of the gold surface, thereby being able to perform up to 20 detections without appreciable loss of sensitivity.

As shown in Fig. 3B), when the ν was gradually increased from 25 to 200 mV s^{-1}, the currents of redox peak and the square roots of ν had good linear relationship, indicating that this electrochemical reaction process on the sensing platform was diffusion controlled. The apparent electroactive surface area of this modified electrode could be described by Randles-Sevcik equation [41]. Thus, the electrochemistry surface area for CMK-3/poly(AC-*co*-MDHLA)/gold was 0.295 cm^2.

$$I_p = 2.69 \times 10^5 A D^{1/2} n^{3/2} \nu^{1/2} C$$

Furthermore, the gold pseudo reference electrode showed a cathodic shift of potential of 205 mV when compared with the Ag/AgCl reference electrode (Fig. 3C)). The pseudo reference electrode was established near the working electrode to minimize ohmic drop effects.

3.3. Optimization of experimental variables

Relevant studies of experimental variables that affect the performance of microfluidic immunosensor for EGFR determination in biological samples were done. For the optimization studies, an EGFR control of 30 ng mL^{-1} was employed.

One of the parameters evaluated was the optimal flow rate, which was determined by employing different flow rates and evaluating the current generated during the immune reaction. As shown in Fig. 4A), flow rates from 1 to 2.5 μL min^{-1} had little effect over immune response and over signals obtained, whereas when

Please cite this article in press as: M. Regiart, et al., Microfluidic immunosensor based on mesoporous silica platform and CMK-3/polyacrylamide-*co*-methacrylate of dihydrolipoic acid modified gold electrode for cancer biomarker detection, Analytica Chimica Acta (2017), http://dx.doi.org/10.1016/j.aca.2017.01.029

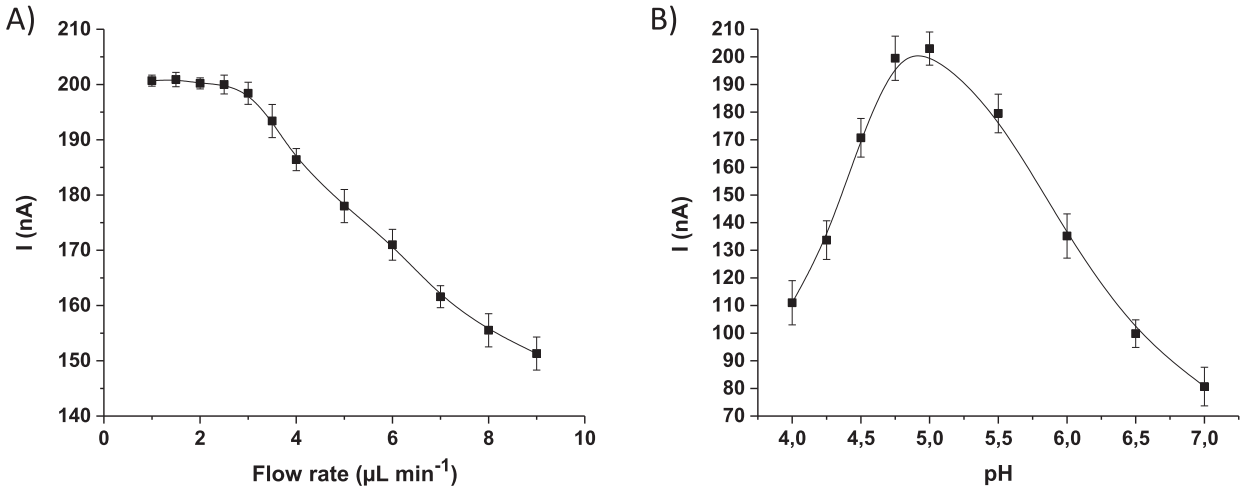

Fig. 4. The dependence of the current produced by the enzymatic response on A) the flow rate effect and B) the pH, using an EGFR control of 30 ng mL^{-1}.

the flow rate exceeded 3 μL min^{-1} the signal was dramatically decreased presumably due to the high flow reduced the time of interaction between the immune reagents. Therefore, a flow rate of 2 μL min^{-1} was used for injections of reagents and washing buffer.

The enzymatic response under flow conditions was analyzed in the pH range of 4.00–7.00 and reached a maximum at pH 5.00. The pH value used was 5.00 in phosphate-citrate buffer (Fig. 4B)). Other parameters like the incubation time between the sample and anti-EGFR, the incubation time of HRP-conjugated anti-EGFR, and the concentration of H_2O_2 and 4-TBC were studied (Fig. A5).

3.4. Analytical performance

Linearity and range of the developed microfluidic immunosensor were studied by analyzing different concentrations (n = 5) of standard solutions containing 0.001–100 ng mL^{-1} of EGFR. A linear relation was observed between the concentration range from 0.01 to 50 ng mL^{-1} as shown in Fig. 3 D. As can be seen, the immunosensor covers the critical concentration range of the EGFR in human serum samples (1–25 ng mL^{-1}) [42].

The calibration curve was described according to the following equation: ΔI (nA) = 77.26 + 4.35 [EGFR] (ng mL^{-1}) with a correlation coefficient of 0.998, where ΔI is the difference between current of the blank and sample (Fig. 3D)). For microfluidic immunosensor and commercial ELISA, the LODs were 3.03 pg mL^{-1} and 1.25 ng mL^{-1}, respectively. The relative standard deviation (RSD) for the determination of 30 ng mL^{-1} EGFR biomarker was 3.81% (n = 5). The precision was evaluated within a single day and over three consecutive days gave RSDs of 4.98% and 5.17%, respectively. Moreover, the microfluidic immunosensor was compared with a commercial ELISA procedure for the quantification of EGFR in five human serum samples under the conditions previously described, while providing a rapid electrochemical readout. The results demonstrated that both methods were statistically equivalent at a confidence level of 95% (Table 2).

Table 3 shows previously published articles for EGFR determination in different human samples such as serum, plasma, and cells. The new method has significant advantages over the previously reported. The present method is a microfluidic immunosensor that use amperometry as detection technique, which offers sensitive determinations in short analysis time, with a low consumption of reagents and samples. Another advantage is the employment of gold electrode modified with a CMK-3/poly(AC-*co*-MDHLA) nanocomposite which provides an increased sensitivity of the system and allows to performed 20 measurements without lost in the sensitivity by avoiding electrode surface fouling.

Furthermore, the achieved LOD is lower than that obtained by the methods recently reported for serum human samples. In addition, our system uses the AMS platform for immobilizing the anti-EGFR antibodies, which provides specificity to the device. Finally, our device has the potential to answer the growing needs for analytical tools that fulfill requirements such as low cost, sensitivity and short analysis time.

Table 3
Comparison with other works using different electrochemical techniques for EGFR determination.

Modification	Electrode	Technique	Sample	Linear range (ng mL^{-1})	LOD (pg mL^{-1})
Ferrocene moiety-peptide ligands [43]	GE[a]	DPV[b]	Serum	0.1–1000	37
Anti-EGFR-dithiobissuccinimidyl propionate [44]	GE	CV	–	0.001–100	1
AuNPs-Protein G-Anti-EGFR [45]	GE	I[c]	Plasma	0.001–1000	0.34
Biotinylated anti-EGFR aptamer-streptavidin magnetic beads. Anti-EGFR-AuNPs [42]	GCE[d]	DPV	Serum	1–40	50
Fe_3O_4/N-trimethyl chitosan/Gold-Anti-EGFR. Polythiophene-Anti-EGFR [46]	SPPE[e]	DPV	Cell	0–1	0.05
CMK-3/poly-(AC-*co*-MDHLA). Anti-EGFR/AMS [this work]	GE	A	Serum	0.01–50	3.03

[a] Gold electrode.
[b] Differential pulse voltammetry.
[c] Impedance.
[d] Glassy carbon electrode.
[e] Screen printed platinum electrode.

Please cite this article in press as: M. Regiart, et al., Microfluidic immunosensor based on mesoporous silica platform and CMK-3/poly-acrylamide-*co*-methacrylate of dihydrolipoic acid modified gold electrode for cancer biomarker detection, Analytica Chimica Acta (2017), http://dx.doi.org/10.1016/j.aca.2017.01.029

4. Conclusions

In this work, we have designed a microfluidic immunosensor for the quantitative detection of EGFR in human serum samples. Our analytical method is based on the covalently immobilization of monoclonal anti-EGFR antibodies on AMS retained in the central channel of a microfluidic device. The overall assay time employed (less than 30 min) was shorter than the time reported for commercial ELISA test kit frequently used in clinical diagnosis (240 min). The microfluidic immunosensor offered several attractive advantages like high stability, high selectivity and sensitivity due to the immobilization of monoclonal antibodies on AMS platform, and the use of CMK-3/poly(AC-*co*-MDHLA) nanocomposite that increase the electroactive surface area. In conclusion, our method could be well suited for biomedical sensing and clinical applications for diagnosis and prognosis of several kinds of epithelial origin carcinomas.

Acknowledgements

The authors wish to thank the financial support from University of Notre Dame, Universidad Nacional de San Luis (UNSL), Instituto de Química de San Luis (INQUISAL), Instituto de Física Aplicada (INFAP), Consejo Nacional de Investigaciones Científicas y Técnicas (CONICET), Agencia Nacional de Promoción Científica y Técnica (ANPCyT) and Fondo para la Investigación Científica y Tecnológica (FONCyT) - PICT-2014-1184, PICT-2013-2407 and PICT-2014-0375.

Appendix A. Supplementary data

Supplementary data related to this article can be found at http://dx.doi.org/10.1016/j.aca.2017.01.029.

References

[1] R.S. Herbst, Review of epidermal growth factor receptor biology, Int. J. Radiat. Oncol. Biol. Phys. 59 (2004) 21–26.
[2] G. Bethune, D. Bethune, N. Ridgway, Z. Xu, Epidermal growth factor receptor (EGFR) in lung cancer: an overview and update, J. Thorac. Dis. 2 (1) (2010) 48–51.
[3] R.B. Cohen, Epidermal growth factor receptor as a therapeutic target in colorectal cancer, Clin. Colorectal Cancer 2 (4) (2003) 246–251.
[4] T.P. Thomas, R. Shukla, A. Kotlyar, B. Liang, J.Y. Ye, T.B. Norris, J.R. Baker, Dendrimer–epidermal growth factor conjugate displays superagonist activity, Biomacromolecules 9 (2) (2008) 603–609.
[5] F. Liu, J. Zhang, Y. Deng, D. Wang, Y. Lu, X. Yu, Detection of EGFR on living human gastric cancer BGC823 cells using surface plasmon resonance phase sensing, Sens. Actuators B Chem. 153 (2011) 398–403.
[6] K. Omidfar, F.S. Amjad Zanjani, A.G. Hagh, M.D. Azizi, S.J. Rasouli, S. Kashanian, Efficient growth inhibition of EGFR over-expressing tumor cells by an anti-EGFR nanobody, Mol. Biol. Rep. 40 (2013) 6737–6745.
[7] K.S. Asgeirsson, A. Agrawal, C. Allen, A. Hitch, I.O. Ellis, C. Chapman, K.L. Cheung, J.F. Robertson, Serum epidermal growth factor receptor and HER2 expression in primary and metastatic breast cancer patients, Breast Cancer Res. 9 (2007) R75.
[8] M.T. Sandri, H.A. Johansson, L. Zorzino, M. Salvatici, R. Passerini, P. Maisonneuve, Andrea Rocca M.D., Giulia Peruzzotti D.Sc, Marco Colleoni M.D., Serum EGFR and serum HER-2/neu are useful predictive and prognostic markers in metastatic breast cancer patients treated with metronomic chemotherapy, Cancer 110 (2007) 509–517.
[9] Y.A. Valentin-Vega, J.A. Barboza, G.P. Chau, A.K. El-Naggar, G. Lozano, High-levels of the p53 inhibitor MDM4 in head and neck squamous carcinomas, Hum. Pathol. 38 (2007) 1553–1562.
[10] J. Thariat, M.-C. Etienne-Grimaldi, D. Grall, R.-J. Bensadoun, A. Cayre, F. Penault-Llorca, L. Veracini, M. Francoual, J.-L. Formento, O. Dassonville, D. De Raucourt, L. Geoffrois, P. Giraud, S. Racadot, S. Morinière, G. Milano, E. Van Obberghen-Schilling, Epidermal growth factor receptor protein detection in head and neck cancer patients: a many-faceted picture, Clin. Cancer Res. 18 (5) (2012) 1313–1322.
[11] F.R. Hirsch, R. Dziadziuszko, N. Thatcher, H. Mann, C. Watkins, D.V. Parums, G. Speake, B. Holloway, P.A. Bunn Jr., W.A. Franklin, Epidermal growth factor receptor immunohistochemistry: comparison of antibodies and cutoff points to predict benefit from gefitinib in a phase 3 placebo-controlled study in advanced nonsmall-cell lung cancer, Cancer 112 (2008) 1114–1121.
[12] S.A. Sarkis, B.H. Abdullah, B.A. Abdul Majeed, N.G. Talabani, Immunohistochemical expression of epidermal growth factor receptor (EGFR) in oral squamous cell carcinoma in relation to proliferation, apoptosis, angiogenesis and lymphangiogenesis, Head. Neck Oncol. 2 (2010) 13–20.
[13] R.C.B. Marques, S. Viswanathan, H.P.A. Nouws, C. Delerue-Matos, M.B. González-García, Electrochemical immunosensor for the analysis of the breast cancer biomarker HER2 ECD, Talanta 129 (2014) 594–599.
[14] U. Eletxigerra, J. Martinez-Perdiguero, S. Merino, R. Barderas, R.M. Torrente-Rodríguez, R. Villalonga, J.M. Pingarrón, S. Campuzano, Amperometric magneto immunosensor for ErbB2 breast cancer biomarker determination in human serum, cell lysates and intact breast cancer cells, Biosens. Bioelectron. 70 (2015) 34–41.
[15] J. Peng, Y. Zhu, X. Li, L. Jiang, E. Abdel-Halim, J. Zhu, Electrochemical immunoassay for the prostate specific antigen using ceria mesoporous nanospheres, Microchim. Acta 181 (2014) 1505–1512.
[16] G.M. Whitesides, The origins and the future of microfluidics, Nature 442 (2006) 368–373.
[17] S.E. Weigum, P.N. Floriano, N. Christodoulides, J.T. McDevitt, Cell-based sensor for analysis of EGFR biomarker expression in oral cancer, Lab. Chip 7 (2007) 995–1003.
[18] S.E. Weigum, P.N. Floriano, S.W. Redding, C.K. Yeh, S.D. Westbrook, H.S. McGuff, A. Lin, F.R. Miller, F. Villarreal, S.D. Rowan, N. Vigneswaran, M.D. Williams, J.T. McDevitt, Nano-bio-chip sensor platform for examination of oral exfoliative cytology, Cancer Prev. Res. (Phila) 3 (4) (2010) 518–528.
[19] N.H. Moreira, A. Luis de Jesus de Almeida, M. Helena de Oliveira Piazzeta, D. Pereira de Jesus, A. Deblire, Â.L. Gobbi, J.A. Fracassi da Silva, Fabrication of a multichannel PDMS/glass analytical microsystem with integrated electrodes for amperometric detection, Lab. Chip 9 (2009) 115–121.
[20] F.C. Moraes, R.S. Lima, T.P. Segato, I. Cesarino, J.L. Melendez Cetino, S.A. Spinola Machado, F. Gomez, E. Carrilho, Glass/PDMS hybrid microfluidic device integrating vertically aligned SWCNTs to ultrasensitive electrochemical determinations, Lab. Chip 12 (2012) 1959–1962.
[21] M. Castaño-Álvarez, M.T. Fernández-Abedul, A. Costa-García, Amperometric PMMA-microchip with integrated gold working electrode for enzyme assays, Anal. Bioanal. Chem. 382 (2005) 303–310.
[22] L.Y. Shiroma, M. Santhiago, A.L. Gobbi, L.T. Kubota, Separation and electrochemical detection of paracetamol and 4-aminophenol in a paper-based microfluidic device, Anal. Chim. Acta 725 (2012) 44–50.
[23] J. Wang, Y. Lin, Functionalized carbon nanotubes and nanofibers for biosensing applications, Trends Anal. Chem. 27 (7) (2008) 619–626.
[24] J. Lu, S. Liu, S. Ge, M. Yan, J. Yu, X. Hu, Ultrasensitive electrochemical immunosensor based on Au nanoparticles dotted carbon nanotube–graphene composite and functionalized mesoporous materials, Biosens. Bioelectron. 33 (1) (2012) 29–35.
[25] X. Bo, W. Xie, J.C. Ndamanisha, J. Bai, L. Guo, Electrochemical oxidation and detection of morphine at ordered mesoporous carbon modified glassy carbon electrodes, Electroanal 21 (2009) 2549–2555.
[26] J.C. Ndamanisha, L.P. Guo, Ordered mesoporous carbon for electrochemical sensing: a review, Anal. Chim. Acta 747 (2012) 19–28.
[27] X. Chen, J. Lawrence, S. Parelkar, T. Emrick, Novel zwitterionic copolymers with dihydrolipoic acid: synthesis and preparation of nonfouling nanorods, Macromolecules 46 (1) (2013) 119–127.
[28] M. Hasanzadeh, N. Shadjou, M. Eskandani, M. de la Guardia, E. Omidinia, Mesoporous silica materials for use in electrochemical immunosensing, Trends Anal. Chem. 45 (2013) 93–106.
[29] M. Yang, H. Li, A. Javadi, S. Gong, Multifunctional mesoporous silica nanoparticles as labels for the preparation of ultrasensitive electrochemical immunosensors, Biomaterials 31 (2010) 3281–3286.
[30] Y. Wu, C. Chen, S. Liu, Enzyme-functionalized silica nanoparticles as sensitive labels in biosensing, Anal. Chem. 81 (2009) 1600–1607.
[31] R.-P. Liang, Z.-X. Wang, L. Zhang, J.-D. Qiu, A label-free amperometric immunosensor for alpha-fetoprotein determination based on highly ordered porous multi-walled carbon nanotubes/silica nanoparticles array platform, Sens. Actuators B Chem. 166–167 (2012) 569–575.
[32] D.C. Duffy, J. Cooper McDonald, O.J.A. Schueller, G.M. Whitesides, Rapid prototyping of microfluidic systems in poly(dimethylsiloxane), Anal. Chem. 70 (1998) 4974–4984.
[33] D. Barrera, M. Dávila, V. Cornette, J.C.A. De Oliveira, R.H. López, K. Sapag, Non-hydrothermal synthesis of cylindrical mesoporous materials: pore size distribution of ordered nanostructured carbon CMK-3 by means of experimental techniques and Monte Carlo simulations, Micropor. Mesopor. Mater. 180 (2013) 71–78.
[34] M. Takara, M. Toyoshima, H. Seto, Y. Hoshino, Polymer-modified gold nanoparticles via RAFT polymerization: a detailed study for a biosensing application, Polym. Chem. 5 (2014) 931–939.
[35] M.A. Einarsrud, M.B. Kirkedelen, E. Nilsen, K. Mortensen, J. Samseth, Structural development of silica gels aged in TEOS, J. Non-Cryst. Solids 231 (1998) 10–16.
[36] J. Sun, D. Ma, H. Zhang, X. Liu, X. Han, X. Bao, G. Weinberg, N. Pfänder, D. Su, Toward monodispersed silver nanoparticles with unusual thermal stability, J. Am. Chem. Soc. 128 (2006) 15756–15764.
[37] S. Brunauer, P.H. Emmett, E. Teller, Adsorption of gasses in multimolecular layers, J. Am. Chem. Soc. 60 (1938) 309–319.
[38] J. Villarroel-Rocha, D. Barrera, A.A. García Blanco, Ma.E. Roca Jalil, K. Sapag, Importance of the αS-plot method in the characterization of nanoporous

materials, Adsorpt. Sci. Technol. 31 (2013) 165–183.
[39] F. Rouquerol, J. Rouquerol, K.S.W. Sing, P. Llewellyn, G. Maurin, Adsorption by Powders and Porous Solids: Principles, Methodology and Applications, Academic Press, San Diego, 2014.
[40] J. Villarroel-Rocha, D. Barrera, K. Sapag, Introducing a self-consistent test and the corresponding modification in the Barrett, Joyner and Halenda method for pore-size determination, Micropor. Mesopor. Mater. 200 (2014) 68–78.
[41] A.J. Bard, L.R. Faulkner, Electrochemical Methods: Fundamentals and Applications, second ed., Marcel Dekker, New York, 2001.
[42] H. Ilkhani, M. Sarparast, A. Noori, S. Zahra Bathaie, M.F. Mousavi, Electrochemical aptamer/antibody based sandwich immunosensor for the detection of EGFR, a cancer biomarker, using gold nanoparticles as a signaling probe, Biosens. Bioelectron. 74 (2015) 491–497.
[43] R. Li, H. Huang, L. Huang, Z. Lin, L. Guo, B. Qiu, G. Chen, Electrochemical biosensor for epidermal growth factor receptor detection with peptide ligand, Electrochim. Acta 109 (2013) 233–237.
[44] A. Vasudev, A. Kaushik, S. Bhansali, Electrochemical immunosensor for label free epidermal growth factor receptor (EGFR) detection, Biosens. Bioelectron. 39 (2013) 300–305.
[45] R. Elshafey, A.C. Tavares, M. Siaj, M. Zourob, Electrochemical impedance immunosensor based on gold nanoparticles–protein G for the detection of cancer marker epidermal growth factor receptor in human plasma and brain tissue, Biosens. Bioelectron. 50 (2013) 143–149.
[46] K. Omidfar, M. Darzianiazizi, A. Ahmadi, M. Daneshpour, H. Shirazi, A high sensitive electrochemical nanoimmunosensor based on Fe3O4/TMC/Au nanocomposite and PT-modified electrode for the detection of cancer biomarker epidermal growth factor receptor, Sens. Actuators B Chem. 220 (2015) 1311–1319.

Please cite this article in press as: M. Regiart, et al., Microfluidic immunosensor based on mesoporous silica platform and CMK-3/poly-acrylamide-*co*-methacrylate of dihydrolipoic acid modified gold electrode for cancer biomarker detection, Analytica Chimica Acta (2017), http://dx.doi.org/10.1016/j.aca.2017.01.029